

Clamshell-type Bis-phthalocyanine with Tetrachlorocyclotriphosphazene Intramolecular Bridge: Synthesis and Structural Evaluation by DFT, NMR and Optical Spectroscopy

Alexander Yu. Tolbin,^{*[a]} Boris N. Tarasevich,^[b] Mikhail K. Beklemishev,^[b] Valery K. Brel,^[c] and Victor E. Pushkarev^[a]

An interaction of 2-hydroxy-9(10),16(17),23(24)-tri-*tert*-butyl-29*H*,31*H*-phthalocyanine (1) with hexachlorocyclotriphosphazene (phosphonitrilic chloride trimer) produced, along with the A₃B type low-symmetry monophthalocyanine (monomer 2), a bis-derivative 3 with spectral characteristics such as that of most clamshell-type phthalocyanines (typically, *H*-dimers). The reaction can be considered conditionally selective. DFT calcu-

lations showed the possibility of the existence of several isomers. Based on the UV-Vis, fluorescent and NMR studies, we found that 3 was obtained as an inseparable mixture of three diastereomers-achiral *cis*-isomer and two chiral *trans*-isomers. DFT analysis has also shown that *cis*-isomer can exist as two rotamers-*parallel* and *oblique*, by an analogy with the cofacial *J*-type dimers that we obtained earlier.

Introduction

Phthalocyanine dimers, in which the macrocycles are arranged cofacially and/or bridged by covalent spacers, demonstrate effective intramolecular π - π interactions and are of interest for the creation of nonlinear optical (NLO) and electrochromic materials, organic light-emitting diodes (OLEDs), field-effect transistors (OFETs), gas sensors, etc.^[1] The mutual binding of two or more macrocycles increases the number of reaction centres and yields improved or novel characteristics. In contrast to the original monomers,^[2] such dimers exhibit unusual electrical and spectroscopic properties. In particular, we have shown that stable supramolecular phthalocyanine slipped-cofacial *J*-dimers reveal nano-aggregation in the solid phase,^[3] exhibit NLO properties, and can be used as low-threshold optical limiters.^[4]

In the present work, we focus on cofacial bis-phthalocyanines, in which the macrocycles are linked by one covalent spacer. In 1984, Prof. Leznoff suggested the term '*clamshell*' for

this type of dyes.^[5] The uniqueness of bis-phthalocyanines with a parallel arrangement of macrocycles lies primarily in the fact that they represent stable *H*-type dimers. As a consequence, they exhibit an additional blue-shifted absorption band in the UV-Vis spectra^[6] and low fluorescence quantum yields due to intramolecular self-quenching between the coupled halves of the dimeric species.^[7] The literature reports on a huge variety of related derivatives.^[8] The chemical and physical properties of clamshell-type phthalocyanines depend on the nature of the bridging groups, which also determine the distance between the face-to-face molecules.^[9] The prospects for using clamshell-type phthalocyanines as a gate dielectric for OFETs with a low leakage current density,^[10] as well as in Schottky barrier diodes^[11] are shown. The complexation of rare earth element ions in the space between the macrocycles of clamshell-type phthalocyanines opens up the possibility for controlling the mutual configuration of macrocycles in sandwich bis-phthalocyanine complexes and, therefore, has allowed fine-tuning their spectral and electrochemical properties.^[12] The presence of intramolecular interactions in cofacial closed conformations of clamshell-type phthalocyanines suppresses intermolecular aggregation, which is highly undesirable for solar cells and photodynamic cancer therapy.^[13] Selective control of the desired photophysical and NLO properties can be based on an increase in the number of peripheral cross-linkages. This leads to an increase in the rigidity of molecules and, as a consequence, enhances the π - π interactions. The first example of a clamshell-type bis-phthalocyanine with four intramolecular covalent bridges (assigned as *ball*-type) was published by us in 2003.^[14] Later, in the group of Prof. Bekaroğlu, various derivatives were obtained, and the prospects for their application as electroluminescent materials were shown.^[15]

In our previous work,^[16] we reported the synthesis of a low-symmetry monophthalocyanine containing one pentachlorocyclotriphosphazene ring at the periphery and showed its ability

[a] A. Y. Tolbin, V. E. Pushkarev
Institute of Physiologically Active Compounds,
Russian Academy of Sciences, 142432 Chernogolovka,
Moscow Region (Russian Federation)
Tel.: +7 496 5242566
E-mail address:
E-mail: tolbin@ipac.ac.ru

[b] B. N. Tarasevich, M. K. Beklemishev
Department of Chemistry M. V. Lomonosov
Moscow State University,
119991 Moscow (Russian Federation)

[c] V. K. Brel
A. N. Nesmeyanov Institute of Organoelement Compounds,
Russian Academy of Sciences,
119991 Moscow (Russian Federation)

Supporting information for this article is available on the WWW under <https://doi.org/10.1002/slct.202201065>

to a photoinduced intramolecular energy transfer from the macrocycle to the phosphazene ring. Due to the presence of active chlorine atoms in this compound, it is possible to obtain bi- and polymacrocyclic derivatives. Such dyes, owing to the presence of the electron-withdrawing phosphazene spacer, in the nearest future could form the basis of new NLO materials for advanced laser technologies. In this work, we report the first synthesis and characterization of *clamshell*-type bis-phthalocyanine, the macrocycles of which are linked by a phosphazene spacer. Note that currently in the literature there are few examples of macrocyclic dyes with cyclotriphosphazene rings at the periphery.^[17]

Experimental

General methods

All solvents were of reagent-grade quality and were obtained directly from Aldrich. Phthalocyanine (Pc) ligands **1**, **2** were synthesized according to our previously published procedures.^[16,18]

UV-Vis spectra were recorded on a Hitachi U-2900 spectrophotometer in a range of 300–1100 nm in tetrahydrofuran (THF). The fluorescence quantum yields (Φ_F) were estimated from the fluorescence emission spectra (Lumex Fluorat-02-Panorama Spectrofluorometer) using Rhodamine 6G as a reference ($\lambda_{\text{ex}} = 340$ nm, $\Phi_F = 0.95$ ^[19]) by the formula (1):

$$\Phi_F^{(x)} = \frac{A_s F_x}{A_x F_s} \cdot \left(\frac{n_x}{n_s} \right)^2 \cdot \Phi_F^{(s)} \quad (1)$$

where Φ_F is the fluorescence quantum yield, A is the absorbance at the excitation wavelength, F is the area under the emission curve, and n is the refractive index of the solvents used. Indexes 's' and 'x' refer to the standard and the unknown substance, respectively.^[20]

FT-IR spectrum of phthalocyanine **3** was obtained in ZnSe pellets on a Nicolet Nexus IR-Furje spectrometer. ¹H and ³¹P{¹H} NMR spectra were recorded using a Bruker AVANCE 500 spectrometer (500.20 MHz and 202.48 MHz for ¹H and ³¹P, respectively) with the samples dissolved in CDCl₃ or DMSO-*d*₆. Triethylamine (NEt₃, 12 vol %) and sodium methylate-*d*₃ (MeONa-*d*₃) were used as disaggregating additives: NEt₃/CDCl₃, MeONa-*d*₃/DMSO-*d*₆ and NEt₃/MeONa-*d*₃/DMSO-*d*₆ systems were applied. MeONa-*d*₃ was prepared immediately before use by adding a small piece of Na metal to methanol-*d*₄ at ambient conditions with the following evaporation of the residual solvent. Chemical shifts for ¹H and ³¹P are given in ppm relative to SiMe₄ and H₃PO₄, respectively.

MALDI-TOF/TOF measurements were performed on a Bruker ULTRAFLEX II TOF/TOF spectrometer using 2,5-dihydroxybenzoic acid (DHB, Aldrich) and α -cyano-4-hydroxycinnamic (HCCA, Aldrich) acid as matrices.

Elemental analyses were performed with a EuroVector EA3100 Series of CHNS-O Elemental Analyzers.

The following software was used: 1) Quantum-chemistry package PRIRODA,^[21] 2) *Geometry Analyzer* Module for EasyQuanto.^[22]

Quantum-chemical calculations

Quantum chemical calculations were performed using density functional theory (DFT). The Perdew–Burke–Ernzerhof (PBE) functional^[23] and PRIRODA software package, supplied with the cc-pVDZ basis set,^[24] were used for the optimization of the model structures corresponding to the dimeric chlorophosphazene-containing metal-free phthalocyanines, as well as for scanning of the potential energy surface (PES) of the macrocycles slippage to estimate the stability of the closed cofacial structures. *Tert*-butyl substituents were replaced with hydrogen atoms to reduce calculation time.

The cross-section surface plot of the 3D PES is made by eliminating the z coordinate (energy) using a numerical algorithm for the 2D transformation matrix. The original 50×50 matrix was obtained by kriging based on the tilting and rotation of the macrocycles (x and y coordinates, respectively), as well as the total energy of the system (z coordinate) during the PES scan. For the projection transformation, a 2D-Gaussian function was used (Eqn. 2):

$$f(x, y) = z_0 + A \exp \left\{ -\frac{1}{2} \left(\frac{x - x_c}{w_x} \right)^2 - \frac{1}{2} \left(\frac{y - y_c}{w_y} \right)^2 \right\} \quad (2)$$

where z_0 is the offset, A is the amplitude, x_c, y_c is the center and w_x, w_y are the x and y spreads of the blob.

Visualization of the optimized structures was performed with the *IQmol* program (<http://iqmol.org>). Structural parameters (distances and angles) were calculated with the *Geometry Analyzer* Module for EasyQuanto^[22] to construct a 3D surface (Figure 2). All the quantum chemical calculations (gas-phase) were performed on an Intel/Linux cluster (Joint Supercomputer Centre of Russian Academy of Sciences-<http://www.jsccl.ru>).

Syntheses

1,1,3,5-tetrachloro-3,5-bis(2-oxy-9(10),16(17),23(24)-tri-*tert*-butylphthalocyaninato)-cyclotriphosphazene (3). To a solution of compound **1** (100 mg, 0.14 mmol) in absolute benzene (5 mL) sodium hydride (10 mg, 0.42 mmol) was added followed by the reaction mixture keeping under reflux for 10 min. After that, a stoichiometric amount of hexachlorophosphazene (48 mg, 0.14 mmol) or intermediate compound **2** (140 mg, 0.14 mmol) were added, and the boiling was continued for 10 and 40 min, respectively. Target compound **3** was obtained in 18% (21 mg) and 63% (74 mg) yields, respectively. After the reactions were finished (UV-Vis control), the solvent was evaporated *in vacuo* followed by fast washing of the residues with methanol and chromatographic purification on Bio-Beads SX-1 (BIORAD®) to separate monomer **2** and dimer **3**. Polymeric by-products were fully excluded. THF was used as an eluent.

Analytical data for 2: MALDI-TOF/TOF (matrix-DHB), ¹H NMR (MeONa-*d*₃/DMSO-*d*₆), ³¹P{¹H} NMR (NEt₃/CDCl₃), UV-Vis (CCl₄, acetone, methanol) and FT-IR (ZnSe) are presented in.^[16] Addition data are as follows. UV-Vis (THF), $\lambda_{\text{max}}/\text{nm}$ (log ϵ): 336 (4.80), 635 (4.64), 658 (4.96), 689 (4.97). Fluorescence data for THF: excitation $\lambda_{\text{max}} = 340$ nm, emission $\lambda_{\text{max}} = 698$ nm, Stokes' shift 9 nm, $\Phi_F = 0.094$.

Analytical data for 3: MALDI-TOF/TOF (no matrix): m/z 1671.4641 [M]⁺, calcd for [C₈₈H₆₂Cl₄N₁₅O₂P₃] 1671.4836; (DHB matrix): m/z 1672.4527 [M+H]⁺, 1679.7561 [M+DHB-2HCl-2Cl-3H]⁺; (HCCA matrix): m/z 1672.5208 [M+H]⁺, 1651.8171 [M-2Cl+2CN+H]⁺. ¹H NMR (NEt₃/MeONa-*d*₃/DMSO-*d*₆, δ/ppm): 9.11–9.29 (group m,

16H, α -H^A), 7.98–8.08 (group m, 8H, β -H^A), 1.70–1.73 (group s, 54H, H^{BU}). ³¹P{¹H} NMR (NEt₃/CDCl₃, δ_p /ppm): 23.41–26.27 (group t, 1P, PCl₂, A) [26.27 (t, PCl₂ of *trans*-isomer/first enantiomer, ²J_{P,P} = 53.2 Hz), 25.90 (t, PCl₂ of *trans*-isomer/second enantiomer, ²J_{P,P} = 54.4 Hz), 23.41 (t, PCl₂ of *cis*-isomer/mesoform/Pc *H*-dimer, ²J_{P,P} = 54.6 Hz)], 13.89–15.20 (m, 2P, PCl(OPc), X₂). UV-Vis (THF), λ_{\max} /nm (log ϵ): 333 (5.07), 630 (4.87), 659 (4.87), 692 (4.76). Fluorescence data for THF: excitation λ_{\max} = 340 nm, emission λ_{\max} = 699 nm, Stokes shift 7 nm, Φ_f = 0.033. FT-IR (ZnSe): 3150 (NH), 2950–2860 (C_{Ar}-H), 1610 (C=N), 1200 (P=N), 1090 (P-O), 1010 (P-O-C_{Ar}). Anal. Calcd. (%) for C₈₈H₈₂Cl₄N₁₉O₂P₃: C 63.20, H 4.94, N 15.91. Found: C 62.85, H 4.99, N 15.79.

All spectra the reader can find in the Electronic Supporting Information.

Results and Discussion

Synthesis and Characterization

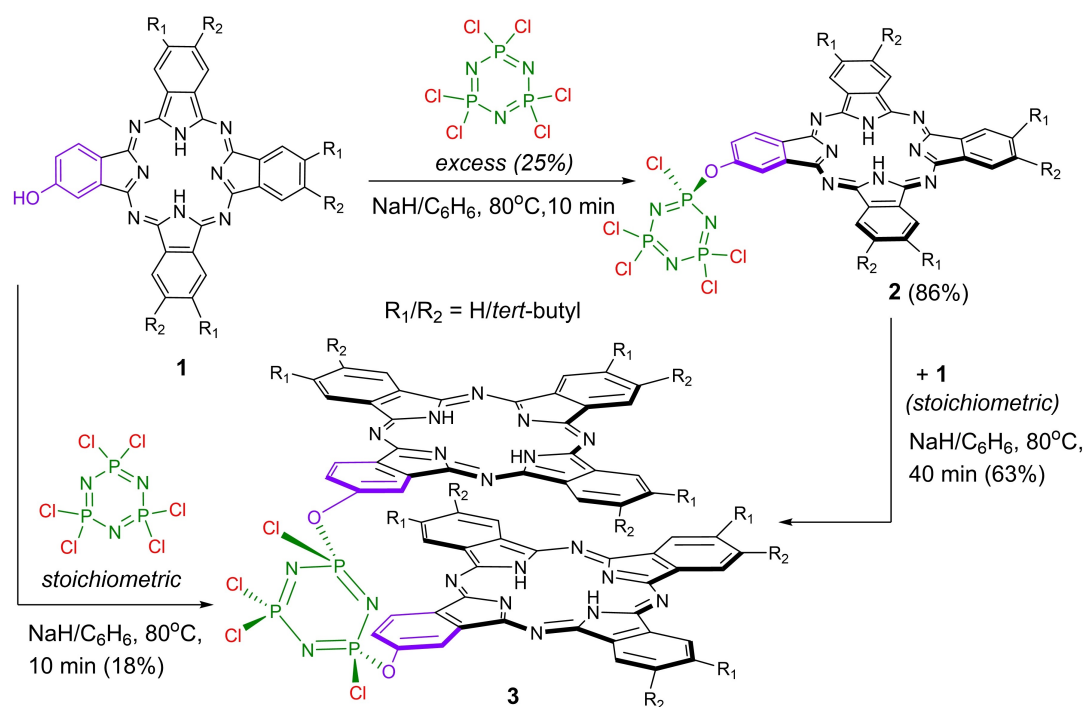
Interaction of asymmetrically substituted phthalocyanine 1^[18] with hexachlorocyclotriphosphazene has resulted in the corresponding functionalized derivatives: monomeric 2 and dimeric 3 dyes (Scheme 1). The high activity of chlorine atoms in the phosphazene ring is the reason for the formation of many polymer by-products during nucleophilic substitution. Earlier, we found that the selectivity in this process is significantly affected by the ratio of reagents and the polarity of the medium.^[16] Thus, with an excess of hexachlorocyclotriphosphazene, mainly monomeric phthalocyanine 2 is formed. Reducing the amount of the reagent requires caution because the selectivity of the reaction is greatly reduced. At a stoichiometric

ratio of 1 and phosphazene without heating, a mixture of oligomeric products is mainly formed. The lack of phosphazene under these conditions leads to incomplete reaction and the formation of a large number of substituted products. An increase in the temperature of the reaction mixture, even with a lack of reagent, makes the reaction conditionally selective with respect to dimer 3, the maximum yield of which drawn up 18%.

Functionalized monophthalocyanine 2 can be considered as an intermediate in the synthesis of target dimer 3. The reaction of phthalocyanines 1 and 2 under the same conditions leads predominantly to binuclear derivative 3. However, steric effects should be considered, which make it difficult to insert the second macrocycle. For this reason, the reaction duration increases.

The formation of by-products is caused not only by the high reactivity of chlorine atoms in the phosphazene ring but also by the destruction of this ring in the presence of a base. Therefore, the contact time should be as short as possible. In this regard, we carried out the selective synthesis of monomer 2 and dimer 3 by keeping the reaction mixtures under reflux in benzene.

Separation of reaction mixtures and isolation of target products 2 and 3 were carried out on a Bio-Beads SX-1 crosslinked polymer. Oligomers were the first to leave the column, then dimer 3 and monomer 2 appeared sequentially. Separation was monitored by UV-Vis and TLC. Sorption carriers such as silica gel are not suitable for the isolation of phosphazene-containing phthalocyanines, because the main amount of them is completely retained at the start of the



Scheme 1. Synthesis of phosphazene-containing monomeric 1 and clamshell-type dimeric 2 phthalocyanine ligands. Conditions: NaH/benzene, 80 °C, 10–40 min.

column. This is due to the interaction of such phthalocyanines with chromatographic support, and this fact itself can be successfully used in the future in the preparation of heterogeneous catalysts and functional nanomaterials.

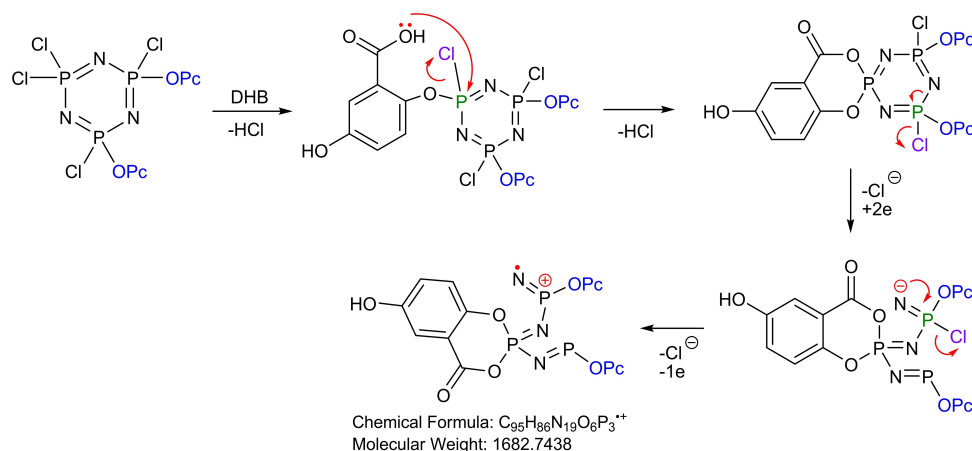
In the MALDI TOF/TOF mass spectrum without a matrix, only the molecular ion peak with m/z 1671.4641 is found (Figure S1-a). No fragmentation is observed, which indicates the high stability of the structure of dye **3** under ionization conditions. However, in the presence of the DHB matrix, an additional peak with m/z 1679.7561 of approximately the same intensity as $[M + H]^+$ appears, which is due to the interaction of the molecular ion with the matrix (Scheme 2, Figure S1-b).

The incorporation of the matrix into structure **3** occurs simultaneously with the successive removal of all chlorine atoms. At the third stage, the breakdown of the phosphazene ring is accompanied by a change in the oxidation state of phosphorus $P(V) \rightarrow P(III)$. This result additionally confirms the high mobility of chlorine atoms in the phosphazene ring. The corresponding secondary ion is absent in both spectra without the matrix and with the HCCA matrix. In the latter case, a secondary ion with m/z 1651.8171 is observed (Figure S1-c), which is due to the replacement of two chlorine atoms by CN groups.

The presence of a phosphazene ring in structure **3** is also confirmed by the FT-IR and ^{31}P NMR spectroscopic study. Thus, the absorption at 1200 cm^{-1} refers to the vibration of the $\text{P}=\text{N}$ bonds. Additional bands at 1010 and 1090 cm^{-1} indicate the fact of binding to phthalocyanine macrocycles (Figure S2). The ^{31}P NMR spectrum of **3** contains signals of both PCl_2 and $\text{PCl}(\text{OPc})$ types in the range of $22\text{--}30$ and $12\text{--}19$ ppm, respectively. In the case of dimer **3**, the signals are resolved worse than that of monomer **2**,^[16] which is associated with strong intramolecular $\pi\text{--}\pi$ interactions of macrocycles. We will give a detailed analysis of the NMR spectra below.

^1H and ^{31}P NMR Spectroscopy

The main peculiarities of the NMR spectroscopy of cyclo-triphosphazene-appended phthalocyanine monomer **2** were discussed in recent short communication,^[16] and herein we further extend this discussion with the data of its dimeric phosphazene-bridged derivative **3**. Thus, both synthesized compounds reveal considerable aggregation in such classical NMR solvents as CDCl_3 and $\text{DMSO-}d_6$ and, consequently, exhibit broadened signals in their ^1H and ^{31}P spectra (Figs. S3–S6). Namely, the proton decoupled ^{31}P spectrum of **2** registered in CDCl_3 (Figure S3) shows the weak unresolved signal of $\text{PCl}(\text{OPc})$ nuclei and the better resolved PCl_2 signals, while the analogous spectrum of **3** (Figure S4) contains poorly resolved signals of both PCl_2 and $\text{PCl}(\text{OPc})$ types. The addition of $1\text{--}2$ vol. % of NEt_3 to the CDCl_3 solutions induces disaggregation, and distinct signals appear in the respective ^{31}P NMR spectra (Figs. S7, S8). As the cyclo-triphosphazene moiety of **2** represents the A_2X spin system, the signal of two PCl_2 nuclei appears as a low-field doublet at 22.45 ppm, and the signal of one $\text{PCl}(\text{OPc})$ nucleus represents a higher-field triplet at 12.60 ppm. In contrast, the cyclo-triphosphazene fragment of **3** is an AX_2 spin system, and both $\text{PCl}(\text{OPc})$ groups in it are stereogenic, anticipating that **3** should exist as a mixture of three stereoisomers (diastereomers)-achiral *cis*-isomer (mesoform) and two chiral *trans*-isomers (enantiomers). As a result, the ^{31}P NMR spectrum of **3** should contain three PCl_2 signals as the low-field triplets and three $\text{PCl}(\text{OPc})$ signals as the higher-field doublets. The actual spectrum recorded in the $\text{CDCl}_3/\text{NEt}_3$ system (Figure S8) indeed contains three low-field PCl_2 triplets in $23\text{--}27$ ppm region with the most intensive one at 23.41 ppm belonging to the *cis*-isomer, while the $\text{PCl}(\text{OPc})$ signals are not fully resolved and are observed as a multiplet in $14\text{--}16$ ppm area. Thus, the ^{31}P NMR spectral data confirm that dye **3** was obtained as an inseparable mixture of stereoisomers, while the integration of signals at 23.41 ppm and $25.63\text{--}26.53$ ppm, respectively, allows determining the approximate *cis*-/*trans*-isomer ratio as $3:2$. Note that the *cis*-isomer of **3** intrinsically should be capable of



Scheme 2. The mechanism of formation of the secondary molecular ion with the participation of the DHB matrix: 'Pc' = phthalocyanine. Statistical analysis of the isotopic splitting of the ultimate ion shows the absence of chlorine atoms.

certain intramolecular π -stacking interactions, which are discussed in the 'UV-Vis and Fluorescence Study' section.

The ^1H NMR spectra of **2** and **3** initially recorded in CDCl_3 solutions (Figures S5, S6) indicate considerable aggregation due to intermolecular stacking interactions between the π -systems of the phthalocyanine rings. Upon NEt_3 addition, the aggregation tendency slightly decreases for **2** (resolution of the signals improves) and, on the contrary, increases in the case of **3** (resolution decreases). Combined with the ^{31}P NMR data, these observations indicate that NEt_3 preferentially solvates phosphazene moieties in **2** and **3**; this solvation enables better resolution in the ^{31}P NMR spectra, but it is insufficient to overcome strong π - π interactions, especially in the case of dimeric ligand **3**. In an attempt to weaken these interactions sufficiently for observation of the resolved proton signals, we decided to apply MeONa-d_3 as a deprotonating agent, which would produce anionic species of the phthalocyanine ligands.

The disaggregating system $\text{MeONa-d}_3/\text{methanol-d}_4$ was recently elaborated in our group to obtain the resolved ^1H NMR spectra of a hydroxy-substituted phthalocyanine ligand and its aluminium complex.^[25] Herein, we modified this system by replacing methanol-d_4 with DMSO-d_6 , as this significantly increased the solubility of dyes **2** and **3**. The resulting spectra of deprotonated **2** and **3** (Figures S9, S10) reveal clear signals of α - and β -type protons in 9 and 8 ppm regions, respectively. The inevitable in such conditions process of gradual substitution of the chlorine atoms at the phosphazene rings by the alkoxy-groups^[26] can be traced by the corresponding changes in the ^{31}P NMR spectra. Thus, using the example of dimeric ligand **3**, the introduction of basic MeONa-d_3 (Figure 1) leads to

a gradual decrease in the intensity of PCl_2 signals and a simultaneous appearance and an increase in the intensity of the signals in 4–10 ppm region, which correspond to double alkoxy-substitution at the phosphorus atom. Notably, the cyclotriphosphazene ring itself remains stable in these conditions at least for several days, which is evidenced by the absence of signals in 0–5 ppm region, as well as in the higher fields, typical for the orthophosphate and other hydrolysis products.

DFT calculations

According to the DFT calculations, up to four isomers are possible for dimeric phthalocyanine **3**. The optimized structures are shown in Figure 2.

*Ips*o- isomer, in which the macrocycles are linked through a common phosphorus atom, represents a partially opened shell with a distance between the centres of the macrocycles of 7.8 Å. This is due to the overly short spacer (3.2 Å), which does not allow macrocycles to accept a parallel arrangement, as is the case for the closed *cis*- isomers. The latter are essentially *parallel* and *oblique* rotamers that can transform into each other by opening/closing the shell while overcoming the 2.1 kcal/mol barrier as shown by the PES scan (Figure 3a).

Due to the small transition apex, the transformation of rotamers into each other can occur freely, but in practice, this means the presence of equilibrium. The transition state is a set of structures with a shifted and opened location of the macrocycles that form a saddle on a PES with a depth of 0.4 kcal/mol (marked in red in Figure 3a). Statistical analysis

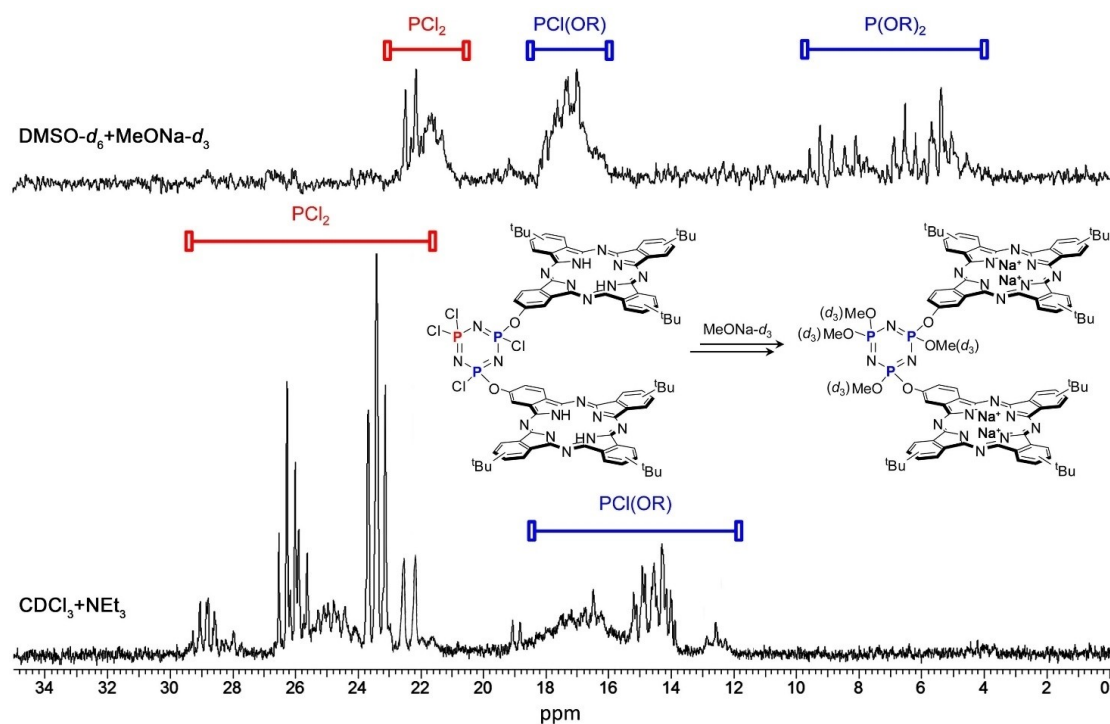


Figure 1. ^{31}P NMR spectra (1024 scans) of **3** (5.77×10^{-2} M) in $\text{MeONa-d}_3/\text{DMSO-d}_6$ system and in CDCl_3 with the addition of 1–2 vol % NEt_3 .

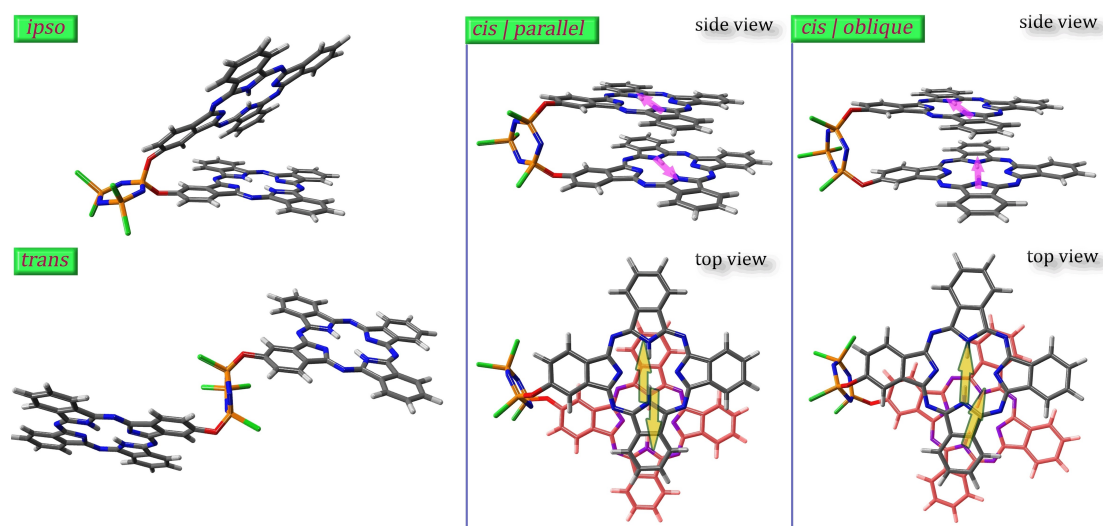


Figure 2. DFT optimized structures (models based on dimeric phthalocyanine **3**): partially-opened shell (*ipso*- isomer), in which macrocycles are joint through common P atom; *clamshell*-type slipped-cofacial with the *parallel* and *oblique* arrangement of the macrocycles (*cis*- isomers), and fully-opened shell representing a *trans*- isomer. The arrows show the vectors drawn through the reference nitrogen atoms in each molecule.

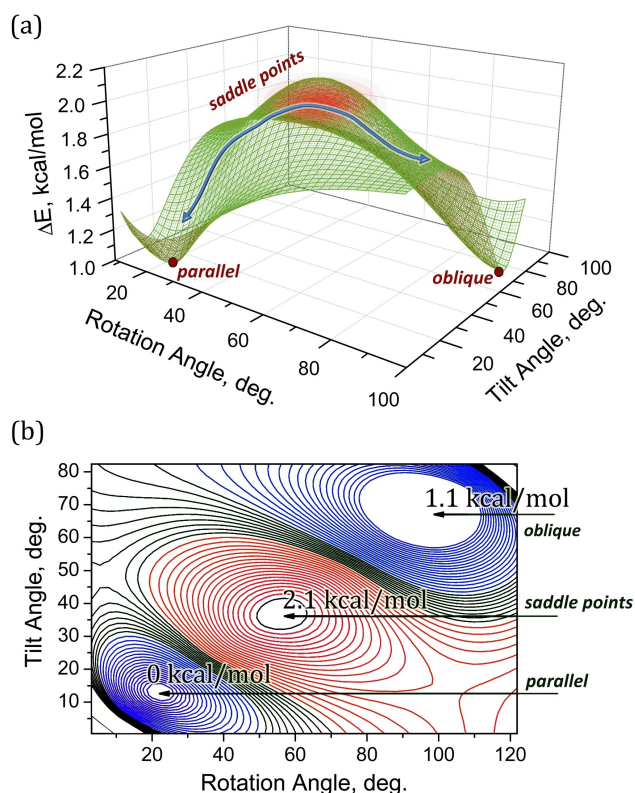


Figure 3. (a) 3D Surface of mutual transformation of *cis*- conformers: *parallel* \leftrightarrow *oblique*; (b) 2D Gauss transformation of the PES showing stable conformational states (Eqn. 2).

(Figure 3b) shows that the number of such structures (stationary points on the PES) is significantly less than for *oblique* type conformers, in which co-facial macrocycles have a sloped orientation (Figure 2: shown by arrows). In turn, the set of

structures corresponding to the *parallel* type *cis*- isomer is the least, or the structure exists in a single kind. Hence, it follows that the equilibrium is likely to be shifted towards the *oblique* conformer. Both of these conformers have no symmetry elements and cannot be unambiguously assigned to any symmetry point group, in contrast to the J-type dimers.^[27]

It is worth noting another important peculiarity. Thus, the P–Cl bond energy in the starting phosphazene is 186 kcal/mol. The inclusion of each successive macrocycle into the structure lowers the energy of the remaining free P–Cl bonds by 10–15 kcal/mol. This implies an equal probability of the formation of all four isomers (Figure 2) and the polymerization priority during the synthesis. However, selectivity in the reaction (Scheme 1) is still achieved, which indicates a significant contribution of the steric factor. Further, we will demonstrate this result using spectroscopic studies.

UV-Vis and Fluorescence Study

The UV-Vis spectra of phthalocyanines **2** and **3** are shown in Figure 4a. Dye **2** is characterized by an absorption spectrum typical for monomeric phthalocyanine ligands to reveal the Soret and Q- (Q_1 , Q_2) bands. In the case of dimer **3**, we observe an additional band at 630 nm which is blue-shifted toward Q-band and can be assigned to an H-band by analogy with the *clamshell*-type binuclear phthalocyanines.^[28] Consequently, dye **3** comprises isomers with a co-facial orientation of the macrocycles, i.e., *cis*- isomers (see Figure 2). The nature of the electronic spectra of **2** and **3** does not change significantly in a wide concentration range from *ca.* 4×10^{-6} to 3×10^{-4} M. Only monomer **2** has some peculiarity: at concentrations above 2.5×10^{-4} M, it tends to form H-dimers (Figure 4c). In our previous work,^[16] we noted that monophthalocyanine **2** is also capable of producing H-type aggregates in methanol.

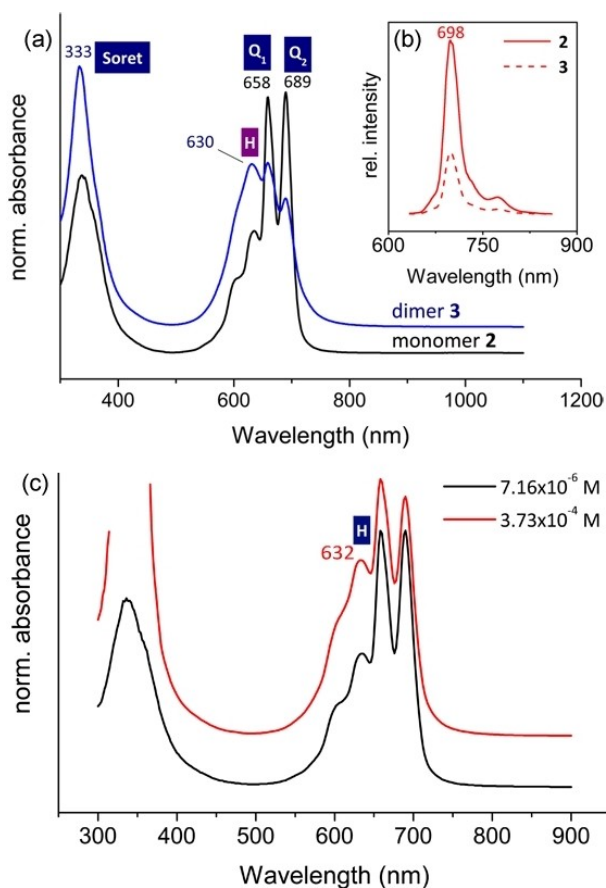


Figure 4. (a) UV-Vis absorption and (b) emission (excitation at 340 nm) spectra. Monomer **2** is about to form *H*-aggregates on increasing the concentration (c).

According to the DFT calculations, the angles between the dipole moments of individual macrocycles in *cis*- conformers (Figure 2) are equal to 52.3 and 46.5 deg. for *oblique* and *parallel* rotamers, respectively. The values of these angles approach the limit of 54 deg., which is the boundary for revealing whether dimers or aggregates belong to the *J*- or *H*-type.^[29] The head-to-head parallel arrangement of the macrocycles and the short distance between them (<3.9 Å) is the reason for the appearance of the intramolecular π - π interactions, which significantly limit conformational equilibria. However, due to the low barrier for the transition of *cis*-conformers into each other (discussed above), there are closed slipped-cofacial *clamshell* structures that should dominate in dynamic equilibria. These structures are represented as the covalently joined *H*-type dimers, which is confirmed by the UV-Vis study.

It is known that *H*-type dimers and aggregates do not produce a fluorescent response.^[30] In the case of dimer **3**, the fluorescence is still observed (Figure 4b), although its quantum yield (Eqn. 1) is approximately three times lower than for monomer **2**. In this case, the positions of the emission bands for both dyes and the Stokes shifts are almost the same. This may be due to the absence of intramolecular vibrational

relaxation, which is characteristic, in particular, of the *J*-type dimers,^[31] in which the macrocycles effectively interact with each other. Consequently, the appearance of a fluorescent response in dye **3** is not associated with the peculiarities of the cofacial arrangement of the macrocycles. This means that along with the *cis*- isomers, which are *H*-type dimers, other isomers can also be formed in the synthesis (Figure 2). In particular, the *trans*- isomer, in which the macrocycles do not have a cofacial arrangement (as shown by the PES scan), should exhibit spectral properties close to the monomer. The formation of the *ipso*- isomer in the synthesis is unlikely both from the point of view of spectral studies and due to the influence of the steric factor, which we have already discussed.

Conclusions

Thus, in the present work, we performed the directed synthesis of the *clamshell*-type bis-(phthalocyanine) **3**, the macrocycles of which are linked through a cyclotriphosphazene spacer. A theoretical analysis of possible bis-macrocylic structures revealed the possibility of the existence of up to four isomers, among which the most probable is the cofacial form with the *cis*- configuration of the macrocycles. For this isomer, it turned out that there are two rotamers: *oblique* and *parallel*, that can easily transform into each other due to the low energy barrier (2.1 kcal/mol), which was shown by PES scanning.

Spectral studies have shown that, along with the *cis*- isomer, the synthesis also provides a certain amount of the *trans*- isomer, which is a mixture of enantiomers. The obtained isomers of dimeric phthalocyanine **3** cannot be separated manually; however, the reaction (Scheme 1) can still be considered selective for the *cis*- isomer, which is a strapped bis-(phthalocyanine) of the *clamshell*-type.

Acknowledgements

The main research concerning synthetic and spectral studies was carried out with the financial support of the Russian Science Foundation (Grant 21-73-20016). The theoretical investigations were performed within the framework of the State Assignment of 2022 (Theme 45.5 Creation of compounds with given physico-chemical properties, N° FFSN-2021-0003). The authors also thank the Joint Supercomputer Centre of RAS (www.jssc.ru) for providing computing resources.

Conflict of Interest

The authors declare no conflict of interest.

Data Availability Statement

The data that support the findings of this study are available in the supplementary material of this article.

Keywords: phthalocyanine · phosphazene · clamshell · *H*-dimer · 3D surfaces · DFT · UV-Vis · ³¹P NMR

- [1] a) M. S. Savelyev, A. Y. Gerasimenko, V. M. Podgaetskii, S. A. Tereshchenko, S. V. Selishchev, A. Y. Tolbin, *Opt. Laser Technol.* **2019**, *117*, 272–279; b) G. Lu, K. Wang, X. Kong, H. Pan, J. Zhang, Y. Chen, J. Jiang, *ChemElectroChem* **2018**, *5*, 605–609; c) X.-W. Sun, P. Zhao, *Chem. Phys. Lett.* **2019**, *724*, 73–79; d) N. Montenegro-Pohlhammer, R. Sánchez-de-Armas, G. Cárdenas-Jirón, C. J. Calzado, *J. Phys. Chem. C* **2019**, *123*, 28359–28369; e) A. Y. Tolbin, M. S. Savelyev, A. Y. Gerasimenko, L. G. Tomilova, N. S. Zefirov, *PCCP Phys. Chem. Chem. Phys.* **2016**, *18*, 15964–15971; f) M. Özdemir, S. Altinisik, B. Köksoy, B. Canımurbey, S. Koyuncu, M. Durmuş, M. Bulut, B. Yalçın, *Dyes Pigm.* **2022**, *200*, 110125.
- [2] İ. Değirmencioğlu, R. Bayrak, M. Er, K. Serbest, *Polyhedron* **2011**, *30*, 1628–1636.
- [3] A. Y. Tolbin, L. G. Tomilova, *Chin. Chem. Lett.* **2017**, *28*, 89–91.
- [4] a) M. S. Savelyev, A. Y. Gerasimenko, V. M. Podgaetskii, S. A. Tereshchenko, S. V. Selishchev, A. Y. Tolbin, *Opt. Laser Technol.* **2019**, *117*, 272–279; b) A. Y. Tolbin, M. S. Savelyev, A. Y. Gerasimenko, L. G. Tomilova, *Chem. Phys. Lett.* **2016**, *661*, 269–273.
- [5] C. C. Leznoff, S. Greenberg, S. M. Marcuccio, P. C. Minor, P. Seymour, A. B. P. Lever, K. B. Tomer, *Inorg. Chim. Acta* **1984**, *89*, L35–L38.
- [6] a) A. Y. Tolbin, V. E. Pushkarev, L. G. Tomilova, N. S. Zefirov, *J. Porphyrins Phthalocyanines* **2017**, *21*, 128–134; b) B. G. Ongarora, Z. Zhou, E. A. Okoth, I. Kolesnichenko, K. M. Smith, M. G. H. Vicente, *J. Porphyrins Phthalocyanines* **2014**, *18*, 1021–1033.
- [7] H. Yoshiyama, N. Shibata, T. Sato, S. Nakamura, T. Toru, *Org. Biomol. Chem.* **2008**, *6*, 4498–4501.
- [8] a) İ. Değirmencioğlu, K. İren, İ. Yalçın, C. Göl, M. Durmuş, *J. Mol. Struct.* **2022**, *1249*, 131599; b) Ü. Demirbaş, H. Yanık, H. T. Akçay, M. Durmuş, O. Bekircan, H. Kantekin, *J. Coord. Chem.* **2022**, *75*, 448–456; c) F. Bächle, C. Maichle-Mössmer, T. Ziegler, *ChemPlusChem* **2019**, *84*, 1081–1093; d) D. Li, X.-Z. Wang, L.-F. Yang, S.-C. Li, Q.-Y. Hu, X. Li, B.-Y. Zheng, M.-R. Ke, J.-D. Huang, *ACS Appl. Mater. Interfaces* **2019**, *11*, 36435–36443.
- [9] E. S. Dodsworth, A. B. P. Lever, P. Seymour, C. C. Leznoff, *J. Phys. Chem.* **1985**, *89*, 5698–5705.
- [10] S. I. Bueyuekeksi, A. Altındal, N. Acar, A. Senguel, *J. Porphyrins Phthalocyanines* **2018**, *22*, 64–76.
- [11] P. R. Sekhar Reddy, V. Janardhanam, K.-H. Shim, S.-N. Lee, A. A. Kumar, V. R. Reddy, C. J. Choi, *Thin Solid Films* **2020**, *713*, 138343.
- [12] V. E. Pushkarev, A. Y. Tolbin, F. E. Zhurkin, N. E. Borisova, S. A. Trashin, L. G. Tomilova, N. S. Zefirov, *Chemistry* **2012**, *18*, 9046–9055.
- [13] L. Li, X. Yin, Z. Chen, S. Ma, X. Zhao, G. Xi, T. Xu, T. Jia, Y. Wang, X. Zhao, *New J. Chem.* **2022**, *46*, 6353–6359.
- [14] A. Y. Tolbin, A. V. Ivanov, L. G. Tomilova, N. S. Zefirov, *J. Porphyrins Phthalocyanines* **2003**, *07*, 162–166.
- [15] a) T. Ceyhan, A. Altındal, A. R. Özkaya, Ö. Çelikbıçak, B. Salih, M. Kemal Erbil, Ö. Bekaroğlu, *Polyhedron* **2007**, *26*, 4239–4249; b) Z. Odabas, A. Altındal, A. R. Özkaya, M. Bulut, B. Salih, O. Bekaroglu, *Polyhedron* **2007**, *26*, 695–707.
- [16] A. Y. Tolbin, V. K. Brel, B. N. Tarasevich, V. E. Pushkarev, *Dyes Pigm.* **2020**, *174*, 108095.
- [17] a) B. Çoşut, S. Yeşilot, M. Durmuş, A. Kılıç, *Dyes Pigm.* **2013**, *98*, 442–449; b) M. Durmuş, S. Yeşilot, B. Çoşut, A. G. Gürek, A. Kılıç, V. Ahsen, *Synth. Met.* **2010**, *160*, 436–444; c) F. Hacivelioglu, M. Durmuş, S. Yeşilot, A. G. Gürek, A. Kılıç, V. Ahsen, *Dyes Pigm.* **2008**, *79*, 14–23.
- [18] A. Yu. Tolbin, V. E. Pushkarev, L. G. Tomilova, N. S. Zefirov, *Mendeleev Commun.* **2009**, *19*, 78–80.
- [19] J. Georges, N. Arnaud, L. Parise, *Appl. Spectrosc.* **1996**, *50*, 1505–1511.
- [20] S. Fery-Forgues, D. Lavabre, *J. Chem. Educ.* **1999**, *76*, 1260.
- [21] D. N. Laikov, Yu. A. Ustynyuk, *Russ. Chem. Bull., Int. Ed.* **2005**, *54*, 820–826.
- [22] A. Yu. Tolbin, The control system of the quantum-chemical calculations-EasyQuanto, Certificate of state registration of computer program No 2015619026 RU). **2015**.
- [23] M. Erznzerhof, G. E. Scuseria, *J. Chem. Phys.* **1999**, *110*, 5029.
- [24] D. N. Laikov, *Chem. Phys. Lett.* **2005**, *416*, 116–120.
- [25] Y. S. Korostei, A. Y. Tolbin, A. V. Dzuban, V. E. Pushkarev, M. V. Sedova, S. S. Maklakov, L. G. Tomilova, *Dyes Pigm.* **2018**, *149*, 201–211.
- [26] D. Davarci, S. Beşli, E. Demirbas, *Liq. Cryst.* **2013**, *40*, 624–631.
- [27] A. Y. Tolbin, V. E. Pushkarev, I. O. Balashova, A. V. Dzuban, P. A. Tarakanov, S. A. Trashin, L. G. Tomilova, N. S. Zefirov, *New J. Chem.* **2014**, *38*, 5825–5831.
- [28] A. Y. Tolbin, V. E. Pushkarev, E. V. Shulishov, L. G. Tomilova, *J. Porphyrins Phthalocyanines* **2012**, *16*, 341–350.
- [29] M. Bayda, F. Dumoulin, G. L. Hug, J. Koput, R. Gorniak, A. Wojcik, *Dalton Trans.* **2017**, *46*, 1914–1926.
- [30] H. M. Baghramyan, C. Ciraci, *Nat. Photonics* **2022**, *11*, 2473–2482.
- [31] A. Y. Tolbin, V. E. Pushkarev, I. O. Balashova, L. G. Tomilova, *Mendeleev Commun.* **2013**, *23*, 137–139.

Submitted: March 17, 2022

Accepted: July 20, 2022